Assessment of Insulin Action on Glucose Uptake and Production During a Euglycemic-Hyperinsulinemic Clamp in Dog: A New Kinetic Analysis

Owen P. McGuinness and Andrea Mari

We evaluated the validity of the traditional method of assessment of the speed of insulin action during a euglycemic-hyperinsulinemic clamp. We first estimated the error of Steele's model on glucose uptake in these experimental conditions. We tested the appropriateness of estimating the half-time of insulin action by expressing the glucose flux changes as a percent of the maximal change (normalization on a 0% to 100% scale). For this purpose, we performed a 390-minute euglycemic-hyperinsulinemic (2 mU · min^{-1} · kg^{-1}) clamp in five chronically catheterized conscious dogs. We used [3-^{3}H]glucose to assess glucose kinetics. We used a novel analysis based on a circulatory model, which allowed us to overcome the limitations of compartmental analysis. We found that the primary effect of insulin (increased from 12.3 ± 1.6 to 104 ± 15 μU/mL) was to increase the whole-body fractional extraction of glucose (3.0% ± 0.3% to 18% ± 2%). Insulin did not alter the mean whole-body artery-vein transit time (3.1 ± 0.2 *v* 2.9 ± 0.4 minutes). In contrast to the assumptions of the Steele model, which assumes that glucose uptake and rate of appearance (Ra) are equal during the clamp, during the initial 30 minutes of the clamp the increase in glucose uptake preceded (by ~4 minutes) the increase in Ra. Thus, during this period uptake exceeded Ra by about 15%. The maximal difference between Ra and uptake (1 to 1.5 mg · min^{-1} · kg^{-1}) occurred approximately 15 minutes after insulin infusion. Finally, to estimate the half-time of the insulin signal that controls glucose uptake and production, we accounted for the nonlinear relationship between insulin concentration and glucose uptake and production. We found that the traditional normalization of the glucose flux changes on a 0% to 100% scale underestimated the half-time of onset of the insulin signal that controls glucose uptake (half-time, 20 *v* 54 minutes) and glucose production (half-time, 25 *v* 39 minutes). Accounting for the nonlinearity of the dose-response curves may thus be of crucial importance in the evaluation of the onset and offset of insulin action.

TO EVALUATE THE EFFECTIVENESS of insulin in normal and pathological states requires that both the ability and speed with which insulin suppresses hepatic glucose production and enhances glucose utilization must be accurately assessed. A classic approach to evaluating the dynamics of insulin action is to perform a euglycemic-hyperinsulinemic glucose clamp and calculate the time course of glucose uptake and production using the simplified equation of Steele.[1] The limitations of the Steele model in assessing glucose production have been evaluated.[2] However, the accuracy of the calculation of uptake and the problem of the assessment of the speed of insulin action from the calculated glucose fluxes have not been addressed.

The issue of the calculation of glucose production during the clamp has been studied in depth and is essentially solved (eg, Bergman et al[2]). It is now generally agreed that reduction of the specific activity changes during the non–steady state improves the accuracy of Steele's model. This condition can be obtained by infusing the tracer at a rate proportional to the expected rate of glucose appearance (Ra).[3] Successful application of this principle to the glucose clamp has allowed accurate determination of the time course of glucose production and assessment of the error of Steele's model in the specific experimental condition (Bergman et al[2] and references therein).

On the other hand, as pointed out recently,[4] assessing changes in whole-body glucose uptake is difficult, and reducing changes in specific activity does not necessarily minimize the error in estimating glucose uptake. In a euglycemic-hyperinsulinemic glucose clamp experiment, in which arterial glucose concentration is held constant, Steele's model assumes that the glucose concentration in the entire glucose distribution volume (ie, glucose mass) is also constant. Thus, glucose uptake can be equated to the total Ra of glucose. This assumption is not necessarily correct. Although the arterial glucose concentration is held constant, the venous (and extracellular) glucose concentration is not constant and will decrease as glucose utilization increases. Thus, the glucose mass may vary despite a constant arterial glucose concentration. The use of more complex two-compartment models does not circumvent this problem. In fact, depending on the model assumptions, these models can yield estimates of uptake that may be greater than, less than, or equal to the glucose Ra.[4] Accurate calculation of the total Ra of glucose may thus be insufficient to calculate glucose uptake correctly with compartmental models. Although it has been suggested that the variation of total glucose mass is small and has little influence on the calculation of uptake,[5] no specific study to substantiate this conjecture has been performed. The impact of this error on the Steele model estimate of glucose uptake in this experimental condition remains to be determined.

Together with the assessment of glucose production and utilization, several studies have attempted to evaluate the speed of the insulin signal that activates glucose uptake and suppresses glucose production.[6-10] Assessment of the speed of the insulin signal is important for the investigation of its temporal relationships with other physiological variables, such as insulin concentration in plasma or lymph.[6,8] Since direct comparison of variables with different scales is not possible, the usual method is to reduce all variables to the same scale. This is achieved by expressing the change in the value of a variable (eg, glucose uptake) at a given time as a percent of the maximal change in

From the Department of Molecular Physiology and Biophysics, Vanderbilt University, Nashville, TN; and the Institute of Systems Science and Biomedical Engineering, National Research Council, Padua, Italy.

Submitted May 8, 1995; accepted April 15, 1997.

Address reprint requests to Owen P. McGuinness, PhD, 702 Light Hall, Department of Molecular Physiology and Biophysics, Vanderbilt University, Nashville, TN 37232-0615.

0026-0495/97/4610-0004$03.00/0

that variable (ie, linear transformation on a 0% to 100% scale).[6-10] This approach is correct only if the variables in question are related by a linear dynamic relationship. The relationships between an increase in insulin concentration and stimulation of glucose uptake or suppression of glucose production are not linear. Thus, linear scaling may lead to an incorrect evaluation of the delays between the observed increases in plasma insulin concentration and the estimated signals that control glucose fluxes (production and uptake). Although this problem may be known in principle, no attempt has been made to quantify the potential error due to an inappropriate assumption of linearity.

In the present study, we assessed glucose uptake during a euglycemic-hyperinsulinemic clamp using a new class of models called circulatory models. This approach allows us to overcome, in part, the limitations of compartmental analysis.[11] In addition, we examined the impact of accounting for the nonlinear relationships between insulin concentration and glucose fluxes on the estimation of the speed of insulin action.

MATERIALS AND METHODS

Experimental Methods

Animal preparations. Experiments were performed in five conscious mongrel dogs (19.9 ± 1.1 kg) receiving a diet consisting of Kal-Kan meat (Vernon, CA) and Wayne dog chow (Purina Mills, St Louis, MO) once daily. The composition of the diet was 52% carbohydrate, 31% protein, 11% fat, and 6% fiber based on dry weight. Two weeks before the experiment, a laparotomy was performed under general anesthesia (acepromazine 0.5 mg/kg and sodium pentobarbital 30 mg/kg). Blood-sampling catheters were inserted into the portal vein and the left major hepatic vein as previously described.[12] In addition, a blood-sampling catheter was inserted into the femoral artery following an incision in the left inguinal area. The catheters were then filled with saline containing heparin (200 IU/mL). The portal and hepatic blood-sampling catheters were exteriorized through the midline incision and placed in a subcutaneous pocket. The arterial blood-sampling catheter was placed under the skin in the inguinal region. All animals had a good appetite (consuming all of the daily ration), normal stools, a hematocrit greater than 38%, and a leukocyte count less than 18,000 · mm^{-3} on the day before the study. The catheters were removed from the respective pockets under local anesthesia (Lidocaine HCL; Abbott, North Chicago, IL) on the day of the study. Angiocatheters were inserted percutaneously into the right cephalic vein for infusion of indocyanine green and [3-^{3}H]glucose, and into the left cephalic vein for infusion of glucose at a variable rate. In addition, an angiocatheter was inserted into a saphenous vein for infusion of insulin.

Protocol. Each experiment consisted of a 150-minute basal period (−150 to 0 minutes) and a 390-minute clamp period (0 to 390 minutes; Fig 1). At −150 minutes, a primed continuous infusion of [3-^{3}H]glucose (56 μCi, 0.46 μCi/min) and a continuous infusion of indocyanine green (0.1 mg · min^{-1} · m^{-2}) were begun. After the basal period at 0 minutes, a constant peripheral infusion of insulin (2 mU · min^{-1} · kg^{-1}) was begun and continued throughout the entire experiment. Arterial plasma glucose was assessed every 5 minutes, and a variable glucose infusion (50% dextrose) was administered to maintain euglycemia. During the clamp period, the tracer infusion rate was modified to create marked changes of tracer concentration to allow identification of a time-varying model of glucose kinetics. The tracer infusion rate was constant for the first 180 minutes of the clamp. At 180 minutes, the exogenous glucose infusate was replaced with a labeled-glucose infusate, the specific activity of which was similar to the plasma glucose specific activity predictable at the end of the basal period, and the constant [3-^{3}H]glucose infusion was discontinued. In this period (180 to 330 minutes), the tracer infusion rate was changed in proportion to the infusion rate of unlabeled glucose. At 330 minutes, a tracer washout period was begun in which the exogenous glucose infusate that contained [3-^{3}H]glucose was replaced by an infusate that did not contain [3-^{3}H]glucose. Frequent arterial blood samples were taken throughout the experiment (~60 samples in 540 minutes). The adopted pattern of tracer infusion created three 30-minute quasi–steady-state periods: a basal period (−30 to 0 minutes) and two insulin-stimulated periods (150 to 180 and 300 to 330 minutes). In the three quasi–steady-state periods, portal and hepatic venous blood samples were also taken every 10 minutes.

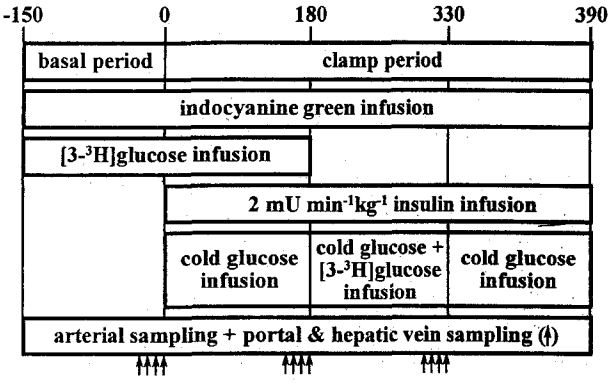

Fig 1. Experimental protocol.

Processing of blood samples. Blood samples were drawn into heparinized syringes and transferred to chilled tubes containing Na_2EDTA (15 mg). Plasma glucose was assayed immediately using a Beckman (Somerset, NJ) glucose analyzer. Immunoreactive insulin[13] was assayed using a Sephadex-bound antibody technique (Pharmacia Diagnostics, Piscataway, NJ; coefficient of variation, 11%). The indocyanine green dye level was measured spectrophotometrically (805 nm) to estimate total hepatic blood flow.[14] Plasma glucose radioactivity was analyzed in duplicate in 1-mL plasma samples that were deproteinized with barium hydroxide (4.5 mL, 0.3N) and zinc sulfate (4.5 mL, 0.3N), evaporated, reconstituted with water (1 mL), combined with scintillation fluid (ACS 10 mL; Amersham, Arlington Heights, IL), and counted on a Beckman scintillation counter (LS9000). Radioactivity (counts per minute) was corrected for quenching. In every study, an internal standard was assayed in triplicate through all of the analysis.

Materials. Porcine insulin was purchased from Eli Lilly and Co (Indianapolis, IN). [3-^{3}H]glucose was purchased from New England Nuclear Research Products (NET-331b; Wilmington, DE). In two studies, high-performance liquid chromatography–purified tracer (NET-331c; New England Nuclear Research Products) was used.

Modeling Analysis

Modeling analysis was based on a circulatory model (Fig 2). The theoretical aspects of this approach, which has its roots in Zierler's studies,[15,16] were studied previously.[11,17,18] Specific mathematical details are reported in the Appendix. The approach is based on the idea of mathematically describing the tracer wave that leaves a vascular bed after a tracer bolus has been injected into an inflowing artery. The shape and magnitude of this wave depends on the properties of tissues within that bed, such as blood flow, fractional extraction of the tracer by the tissues, and volume of distribution. The tracer wave that leaves the vascular bed, scaled to account for tracer dose and blood flow, is called the single-pass impulse response (SPIR) of that bed or tissue. Not only a single organ but also the aggregate of all body tissues can be characterized using the SPIR. In the case of the whole body, the vascular bed includes all vascular beds between the aorta and the right atrium.

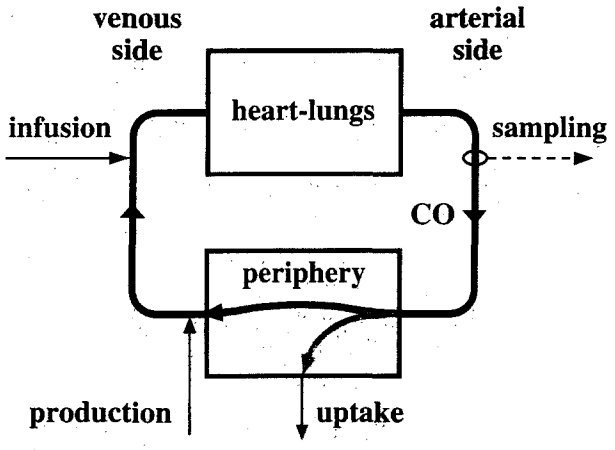

Fig 2. Circulatory model of whole-body glucose kinetics. CO, cardiac output.

Thus, this approach can also be used to study whole-body kinetics, if the recirculation of blood from the right atrium to the aorta is accounted for with a circulatory model.

Model structure. In the circulatory model (Fig 2), body tissues are lumped into two blocks. The heart chambers and lungs are included in the heart-lung block (Fig 2, upper block). The remaining tissues (including heart tissue nourished by the coronary circulation) are included in the periphery block (Fig 2, lower block). For both blocks, blood flow is equal to cardiac output. In the experimental configuration adopted here, labeled and unlabeled glucose are infused at the venous site and sampling takes place at the arterial site.

As already mentioned, the SPIR of the body tissues (periphery block) is the time course of tracer concentration that could be measured in the right atrium after administering a tracer bolus into the left ventricle in an ideal experiment in which recirculation of tracer is prevented. In a classic whole-body tracer experiment, as used in our study, the measured whole-body tracer disappearance curve results from the interaction between SPIRs of the periphery and the heart-lung blocks as the tracer recirculates. This interaction can be described mathematically with a circulatory model. Since the SPIR of the heart-lung block can be predicted (description follows) and it is not altered by insulin, the SPIR of the peripheral tissues and the impact of insulin on those tissues can be determined from the whole-body tracer disappearance curve using the circulatory model.[18]

With our experimental configuration, two assumptions were necessary to determine the SPIR.[18] First, cardiac output was fixed to a constant value of 120 $mL \cdot min^{-1} \cdot kg^{-1}$ based on a compilation of studies.[19] In humans, cardiac output increases slightly (~10%) at insulin levels comparable to those of our experiments,[20] but this was not observed in the dog (D. Wasserman, personal communication, June 1995). Second, we assumed that the SPIR of the heart-lung block [$r_{lung}(t)$] was known and was not affected by insulin. The SPIR of the heart-lung block was modeled as a two-exponential function starting from zero as in experimentally derived curves.[21] We assumed that glucose extraction by the heart-lung block was negligible, and the volume of this block (lungs plus heart chambers) was 17 mL/kg body weight.[21-23]

The SPIR of the periphery block [$r_{per}(t)$] was modeled as a three-exponential function starting from zero, rapidly increasing to a peak, and gradually returning to zero. The exponent determining the initial increase in $r_{per}(t)$ was fixed as in the heart-lung block. The remaining parameters (four) were estimated from the tracer data. During the non–steady state phase of the clamp, the parameters of the periphery block and thus the shape of $r_{per}(t)$ were allowed to change with time.

The impulse responses of the heart-lung and periphery blocks were represented using differential equations (two for heart-lung block and three for periphery block). The combination of these differential equations describes the circulatory model of Fig 2. The model-predicted tracer concentration was obtained by numerical simulation of the differential equations, and the model parameters and $r_{per}(t)$ were estimated by least squares from the measured tracer concentration. Details are given in the Appendix.

Kinetic parameters. The classic concepts of organ kinetics[24] apply to the artery-vein impulse response of the body tissues, $r_{per}(t)$. We calculated from the model parameters the whole-body glucose fractional extraction (dimensionless or percent), ie, 1 − area under $r_{per}(t)$; the glucose clearance ($mL \cdot min^{-1} \cdot kg^{-1}$), ie, the product of fractional extraction and cardiac output; the artery-vein transit time density function, ie, $r_{per}(t)$ normalized to its area; and the mean artery-vein transit time (minutes). Although all of these parameters changed with time during the non–steady state phase of the clamp, the most relevant time-varying parameter was the fractional extraction (or glucose clearance).

Distribution volume. The theoretical aspects of the calculation of the total glucose volume of distribution were considered in detail in a previous report,[17] and will be briefly summarized here. The first point to recall is that with a tracer it is not possible to calculate a physical glucose distribution space but only an "apparent" volume,[24] because glucose is not uniformly distributed in the body water space. The apparent volume is the ratio between the actual tracer mass physically present in the system and arterial tracer concentration.[17,24] Although it would be less ambiguous to consider masses instead of volumes, the traditional use of volumes is preferable because the total glucose mass is dependent on arterial concentration.

To appreciate how the glucose volume of distribution in each of the blocks in Fig 2 is calculated, one should think of an imaginary tracer perfusion experiment. In this experiment, the tracer is first infused in the artery entering the periphery block at a constant rate until complete equilibrium is obtained. Recirculation of tracer from the vein to the artery is prevented. Subsequently, the tracer infusion is stopped, and the tracer mass accumulated in the equilibration phase is either washed out into the venous circulation or taken up by the tissue. The mass of tracer that exits from the tissue divided by the arterial tracer concentration is denoted as *circulating* volume. The mass of tracer that is taken up and metabolized by the tissue divided by the arterial tracer concentration is denoted as *noncirculating* volume.[17] Their sum is the total distribution volume (V_{TOT}). The product of V_{TOT} and arterial glucose concentration is the actual total glucose mass.

The volume components can be calculated from the impulse responses. However, besides the artery-vein impulse response, $r_{per}(t)$, the artery-uptake impulse response must be considered (Fig 2). The artery-uptake impulse response represents the dynamic properties of the movement of glucose from the vascular space into the cell, where the glucose tracer is removed by phosphorylation. Glucose that is removed from the vascular space is not immediately metabolized. There is a delay, as there is for tracer that passes from artery to vein. The expression for the total volume of distribution is an extension of the classic equation for the calculation of volumes.[15] The following equation accounts for the fact that the glucose tracer can leave the tissue by one of two paths (entering the vein or glycolysis)[17]:

$$V_{TOT} = CO \times [(1 - E) \times MTT_{AV} + E \times MTT_{AU}]. \quad (1)$$

In this equation, CO is the cardiac output, E is the fractional extraction, and MTT_{AV} and MTT_{AU} are the mean artery-vein and artery-uptake transit times, respectively. Eq 1 includes the two volume components, ie, the circulating [$CO \times (1 - E) \times MTT_{AV}$] and noncirculating [$CO \times E \times MTT_{AU}$] volume. Note that for unextracted substances

(E = 0), Eq 1 reduces to the classic equation for the volume (volume = flow × mean transit time).

With our glucose tracer ([3-^{3}H]glucose), irreversible glucose uptake is basically equal to the rate of glucose phosphorylation. Thus, the artery-uptake impulse response describes the dynamic relationship between the arterial glucose influx and the rate of glucose phosphorylation. Since glucose is present as free glucose before it is phosphorylated, the total glucose mass is in our context equal to the total free glucose mass (vascular, interstitial, and intracellular). Therefore, in our experiments, V_{TOT} is the ratio between total whole-body free glucose mass and arterial glucose concentration.

The whole-body circulating volume, ie, the sum of the circulating volume of the periphery and of the heart-lung system, is readily calculated because E and MTT_{AV} can be determined from $r_{per}(t)$. This volume equals the noncompartmental estimate of the distribution volume.[17] Unfortunately, the noncirculating volume cannot be calculated, because MTT_{AU} is indeterminable and it is not possible to derive MTT_{AU} from MTT_{AV} without additional experimental information. Thus, we could not experimentally assess the total glucose distribution volume, V_{TOT}.

Calculation of uptake. The calculation of uptake in non–steady state was considered in detail[11] with reference to the model of Fig 2. It was shown that the calculation of uptake requires knowledge of the artery-uptake impulse response (Fig 2), which cannot be obtained from a classic whole-body tracer experiment. To circumvent this problem, calculation of uptake is divided into two steps. In the first step, a substitute for uptake, called arterial-equivalent uptake, is calculated as the product of arterial concentration and clearance. Clearance varies with time and is estimated with the circulatory model from the tracer data. No assumptions on the artery-uptake impulse response are required to calculate arterial-equivalent uptake. However, arterial-equivalent uptake is not equal to uptake. There is a delay as glucose moves from the arterial blood to the glucose-metabolizing cells where it is phosphorylated. In the second step, this delay is taken into account. Theoretically, uptake could be obtained from the convolution of arterial-equivalent uptake with the artery-uptake transit time density function, if this were known. In practice, uptake can be predicted qualitatively as arterial-equivalent uptake delayed by the mean artery-uptake transit time.[11]

An estimate of the mean artery-uptake transit time was derived by combining results from published studies and relationships between variables depicted in Eq 1. We considered that during a euglycemic glucose clamp a change of the total whole-body free glucose mass is not expected if the free glucose content in muscle, which is the most important site of insulin action, does not vary. Since there is no evidence of a change in the muscle nonphosphorylated glucose content (extracellular + intracellular) in man[25-27] and in rat (D. Wasserman, personal communication, June 1995), the total whole-body free glucose mass is not expected to change under the action of insulin. Since V_{TOT} is the ratio of the total whole-body free glucose mass and arterial glucose concentration, which is constant during the clamp, this implies that V_{TOT} (Eq 1) must be constant as well. In our experimental conditions, cardiac output does not change, and we also found experimentally that MTT_{AV} did not change despite a marked increase in the fractional extraction (E). Based on Eq 1, if MTT_{AU} is much greater than MTT_{AV}, when fractional extraction (E) increases V_{TOT} must increase as well, which is in contrast to our observations. On the contrary, if MTT_{AV} equals MTT_{AU}, Eq 1 yields $V_{TOT} = CO \times MTT_{AV}$, which is in our experimental conditions virtually constant. It can thus be conjectured that MTT_{AV} and MTT_{AU} are similar. Therefore, we used the computable MTT_{AV} as an estimate of the noncomputable MTT_{AU}.

Calculation of Ra. In our experiments, the measured glucose concentration is the sum of two components: an endogenous component arising from endogenous glucose production, and an exogenous component arising from infusion of exogenous glucose during the clamp. Using the circulatory model and the tracer-determined parameters, we first calculated the exogenous component of glucose concentration from the known glucose infusion rate. We then subtracted these calculated values from the measured glucose concentration, thus obtaining the endogenous component. Finally, from the endogenous glucose concentration component and using the circulatory model, we calculated glucose production by deconvolution (see the Appendix for details). The total Ra of glucose was obtained as the sum of glucose production and exogenous glucose infusion.

Steele's model. In our analysis, we did not calculate glucose fluxes using Steele's model. This calculation would have been unreliable because of the large changes in specific activity observed in our experiments. We instead evaluated the error of Steele's model on glucose uptake in the ideal situation of constant specific activity. In this condition, the Ra of glucose is accurately calculated.[3] Moreover, in our experimental conditions, glucose uptake as calculated by Steele's model equals the Ra of glucose, because arterial glucose concentration is constant. Thus, the difference between the actual rates of glucose uptake and appearance is the error on glucose uptake of Steele's model in the ideal condition of constant specific activity. We have evaluated this difference with the circulatory model.

Evaluation of Insulin Action

The traditional method for assessing the speed with which insulin stimulates glucose uptake and suppresses glucose production is based on normalization of fluxes on a 0% to 100% scale (linear scaling). For instance, one calculates the ratio between the glucose uptake increment from basal at a given time and the maximal glucose uptake increment. This approach is useful for comparing the time course of two variables measured in different units, in which one (eg, glucose uptake) is supposed to be the effect of the other (eg, insulin concentration in some body compartment). However, linear scaling is misleading if the relationship between the two variables is not linear. This is the case for insulin concentration and glucose uptake, as the latter does not increase in proportion to the former at high insulin concentrations (glucose uptake saturates at high insulin levels).

Consider, for instance, the relationship between insulin concentration at the cell membrane and glucose uptake. Consider first an experiment in which a small gradual increase of insulin concentration at the cell membrane is produced. Suppose that in this experiment both insulin concentration at the cell membrane and glucose uptake reach their half-maximal value at 20 minutes. Consider then a similar experiment at a much higher insulin dose, in which glucose uptake saturates, and suppose that insulin concentration at the cell membrane still reaches its half-maximal value at 20 minutes. In the second experiment, at 20 minutes insulin concentration at the cell membrane is much higher than in the first experiment, but because glucose uptake becomes saturated at this insulin concentration, at 20 minutes glucose uptake is closer to its maximal value, ie, beyond the half-maximal value. The half-time of glucose uptake as calculated by linear scaling must thus be less than 20 minutes. If the speed of insulin action is evaluated using linear scaling, the investigator may have the false impression that increasing the insulin dose also produces an increase of the speed of action. This is not true, since the half-time of the signal that stimulates glucose uptake (ie, insulin concentration at the cell membrane) is 20 minutes in both experiments.

We attempted to overcome this problem by accounting for the saturation of glucose fluxes. We first determined the steady-state relationship between insulin concentration and glucose uptake and production by fitting to the published experimental data[28] and to our results the function,

$$F = F_0 + \frac{E_{max} I}{EC_{50} + I}, \qquad (2)$$

where F is the glucose flux (uptake or production) at a given insulin concentration I, F_0 is the extrapolation of F to zero insulin, E_{max} is the maximal flux, and EC_{50} is the insulin concentration at which the flux is half-maximal. We obtained two distinct sets of parameters (F_0, E_{max}, and EC_{50}) for describing the insulin uptake and insulin production dose-response curves. We then solved Eq 2 for I, and calculated the time course of the insulin concentration, I(t), corresponding to the model-determined glucose flux, F(t) (uptake or production). This calculated (ie, not measured) insulin concentration represents the signal that stimulates glucose uptake (or suppresses glucose production), and is referred to as the "insulin signal." The insulin signal would be the insulin concentration at the cell membrane in the example above. Finally, we plotted the insulin signal on a 0% to 100% scale, and estimated the half-times graphically from the plots.

Arteriovenous Differences

In the three quasi–steady-state periods (−30 to 0, 150 to 180, and 300 to 330 minutes), hepatic glucose uptake and production were calculated with the arteriovenous-difference method. Net hepatic glucose balance (NHGB) was calculated with the equation, $NHGB = 0.73 \times [(0.2G_A + 0.8G_P) - G_H] \times HBF$, where G_A, G_P, and G_H are plasma glucose concentrations in the femoral artery, portal vein, and hepatic vein, respectively, and HBF is hepatic blood flow. The factors 0.2 and 0.8 represent the percent contribution of the hepatic artery and portal vein, respectively, to total hepatic blood flow.[29] The factor 0.73 converts plasma glucose concentrations into blood glucose concentrations.[12] Hepatic tracer uptake (HTU) was calculated as $HTU = 0.73 \times [(0.2G_A^* + 0.8G_P^*) - G_H^*] \times HBF$, where G_A^*, G_P^*, and G_H^* are plasma [3-^{3}H]glucose concentrations in the femoral artery, portal vein, and hepatic vein, respectively. Hepatic glucose uptake (HGU) was calculated by dividing HTU by the average inflowing specific activity, ie, $(0.2G_A^* + 0.8G_P^*)/(0.2G_A + 0.8G_P)$. Hepatic glucose production was calculated as HGU − NHGB.

Data Presentation

The data and results are presented as the mean ± SE. Glucose fluxes, which are piecewise constant functions of time calculated every 10 minutes, are plotted with linearly interpolated lines. The calculated values are drawn centered in the 10-minute interval to which they refer. The Student *t* test was used for the comparisons.

RESULTS

Data and Model Fit

Arterial plasma insulin levels increased from 12.3 ± 1.6 to 104 ± 15 μU/mL following insulin infusion. The exogenous glucose infusion rate required to maintain arterial glycemia constant continuously increased. The mean glucose infusion rates during the quasi–steady-state periods of the clamp (150 to 180 and 300 to 330 minutes) were 13.4 ± 0.9 and 15.2 ± 2.2 $mg \cdot min^{-1} \cdot kg^{-1}$, respectively. Mean arterial plasma glucose and [3-^{3}H]glucose concentrations are shown in Fig 3, together with the model fit. During the clamp, the arterial tracer concentration after the initial decrease followed the pattern of tracer infusion. Since euglycemia was maintained, arterial specific activity followed a pattern similar to that of the tracer.

The mean model residuals (measured − model-predicted concentration) for glucose, [3-^{3}H]glucose, and glucose specific activity did not differ significantly from zero, on average. At most of the time points, the mean residual differed from zero by less than 2 SE of the residual at the given time point. In the basal state, in which standard least squares were used, the coefficients

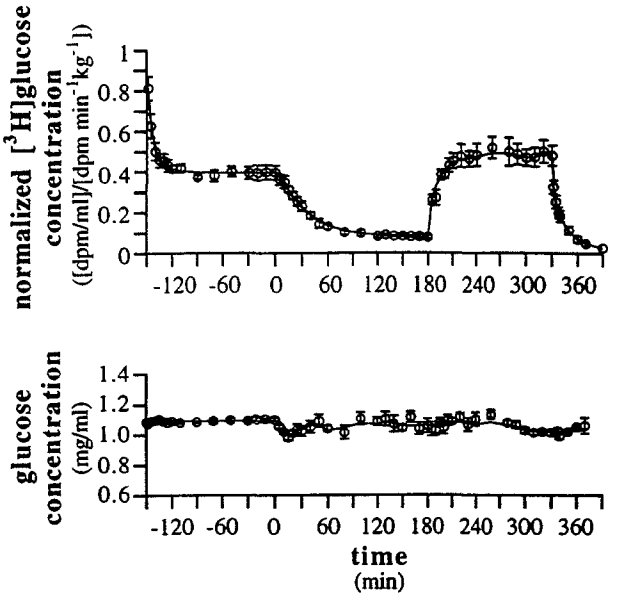

Fig 3. (Top) [3-^{3}H]glucose concentration normalized to the [3-^{3}H]glucose infusion rate of the basal period. (Bottom) Glucose concentration. Solid lines represent the model fit.

of variation of the individually estimated model parameters were less than 25%. We could not calculate the coefficients of variation during the non–steady state, because in this period we did not use standard least squares (see the Appendix). The absence of bias in the residuals and the satisfactory values for the coefficients of variation indicated that the model was of adequate complexity. The model fit was not improved by increasing the number of exponentials of the periphery-block response (results not shown).

Steady-State Parameters

The transit time density functions of the body tissues in the basal (−150 to 0 minutes) and insulin-stimulated (330 to 390 minutes) state are shown in Fig 4. The kinetic parameters (fractional extraction, clearance, mean artery-vein transit time, and circulating volume) are reported in Table 1. The increase of fractional extraction and clearance and the decrease of circulat-

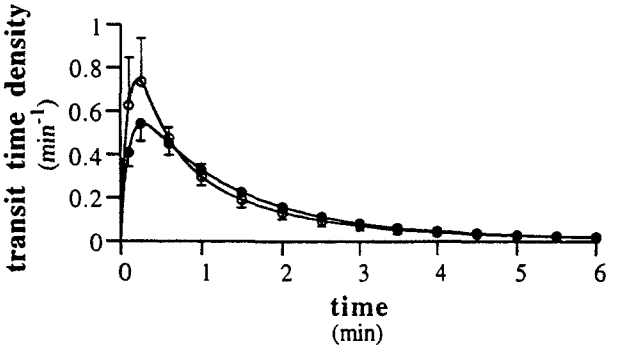

Fig 4. Transit time density function of the body tissues [$r_{per}(t)$ normalized to its area] in the basal (●) and insulin-stimulated (○) steady state. Error bars for the 2 curves are reported at selected times for clarity and drawn in opposite directions.

Table 1. Steady-State Kinetic Parameters of the Periphery

Parameter	Basal (−150 to 0 min)	Insulin-Stimulated (330 to 390 min)
Fractional extraction (%)	3.0 ± 0.3	18 ± 2*
Mean artery-vein transit time (min)	3.1 ± 0.2	2.9 ± 0.4
Clearance (mL · min^{-1} · kg^{-1})	2.6 ± 0.3	16 ± 2*
Circulating volume (mL/kg)	262 ± 18	206 ± 22*

*$P \leq .05$, insulin-stimulated *v* basal.

ing volume were statistically significant. The principal effect of insulin glucose kinetics was to enhance the fractional extraction of glucose in the body tissues. The change in mean artery-vein transit time was not statistically significant, and thus the decrease of circulating volume was a consequence of the increase in fractional extraction (Eq 1). In the insulin-stimulated state, we found a positive correlation between fractional extraction and mean artery-vein transit time ($r = .93$, $P < .05$) and between clearance and circulating volume ($r = .91$, $P < .05$).

Non–Steady-State Calculations

During the non–steady-state period, the fractional extraction of glucose by the body tissues increased from a basal value of 3.0% ± 0.3% to a final value of 18% ± 2% (Table 1). The greatest change occurred in the first 30 minutes, but fractional extraction continued to increase throughout the experiment, as did the exogenous glucose infusion. Glucose arterial-equivalent uptake, total Ra, and production estimated using the circulatory model are reported in Fig 5. The time course of fractional extraction was similar (in its own scale) to that of arterial-equivalent uptake, since arterial glucose concentration was kept constant. The insulin-induced increase in arterial-equivalent uptake preceded the increase in the total Ra by about 7 to 8 minutes (Fig 5, top). The difference between the arterial-equivalent uptake and the Ra was positive in the first 30 minutes (Fig 5, bottom). To determine if this finding could be due to the small initial decrease in glucose concentration (Fig 3), we recalculated the difference between arterial-equivalent uptake and total Ra with the model fixing the glucose concentration during the clamp to the basal value. The peak difference did not change substantially (Fig 5, bottom). We could not calculate the exact time course of uptake. However, we estimated the delay between uptake and arterial-equivalent uptake, ie, the mean artery-uptake transit time, which equals the mean artery-vein transit time (~3 minutes; Table 1). We thus found that the increase in uptake followed the increase in arterial-equivalent uptake by approximately 3 minutes. Since arterial-equivalent uptake preceded the increase in the Ra of glucose by about 7 to 8 minutes, the increase in uptake preceded the increase in the glucose Ra by about 4 to 5 minutes. The peak difference between uptake and total Ra of glucose was estimated to be 1 to 1.5 mg · min^{-1} · kg^{-1}. Glucose production was gradually suppressed to 28% ± 10% of the basal value (Fig 5, middle).

Insulin Action

Figure 6 shows dose-response curves used in calculation of the insulin signal. The estimated parameters of Eq 2 were F_0 = −0.83 mg · min^{-1} · kg^{-1}, E_{max} = 22.2 mg · min^{-1} · kg^{-1}, and EC_{50} = 52.7 μU/mL for uptake and F_0 = 3.42 mg · min^{-1} · kg^{-1}, E_{max} = −3.59 mg · min^{-1} · kg^{-1}, and EC_{50} = 55.6 μU/mL for production. The apparently inconsistent negative value of F_0 (flux at zero insulin, Eq 2) for the uptake dose-response curve is not relevant in our analysis, because the dose-response curve is not used to predict uptake at insulin levels less than basal. The negative F_0 value improved the data fit in the range of insulin concentrations seen in our experiments.

We accounted for the nonlinearity of the insulin concentration–glucose uptake relationship by converting a given glucose flux to an insulin signal with Eq 2. This nonlinear transformation markedly affected the half-times for insulin's effects on glucose production and arterial equivalent-uptake when it was compared against standard linear transformation (Fig 7). For arterial-equivalent uptake, the half-times estimated graphically from Fig 7 were 20 and 54 minutes with linear and nonlinear transformation, respectively. The corresponding values for production were 25 and 39 minutes. Although the half-time for uptake calculated with nonlinear transformation was higher than the half-time for production, the comparison between the speed of uptake activation and production suppression was difficult to assess because the shapes of the curves were different.

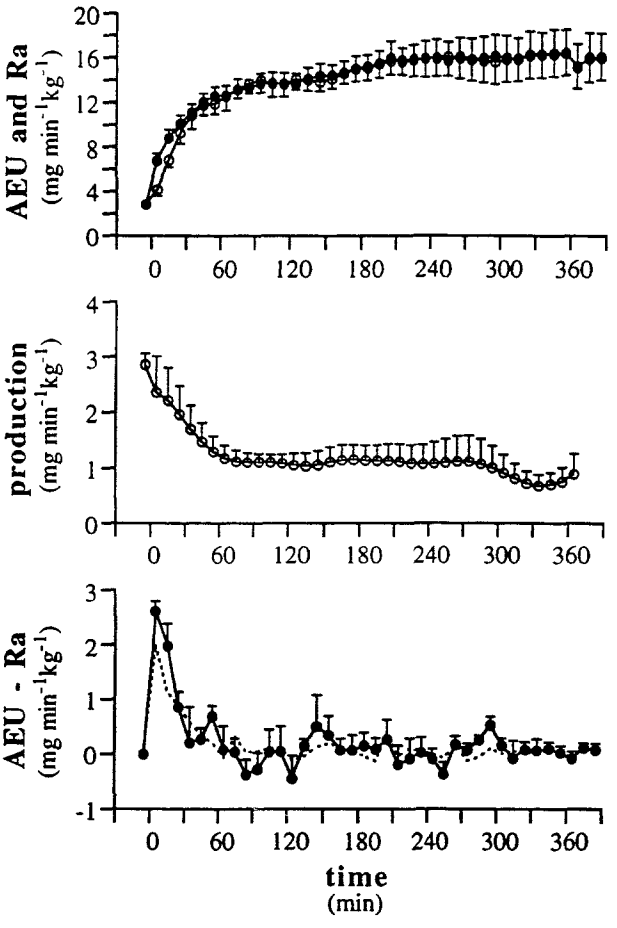

Fig 5. (Top) Glucose arterial-equivalent uptake (AEU, ●) and total Ra (○). Error bars are drawn upward for AEU and downward for Ra. (Middle) Glucose production. (Bottom) Difference between AEU and Ra. Dotted line represents the mean difference calculated with the model and the arterial glucose concentration fixed at its basal value. Basal values are depicted at t = −5 minutes.

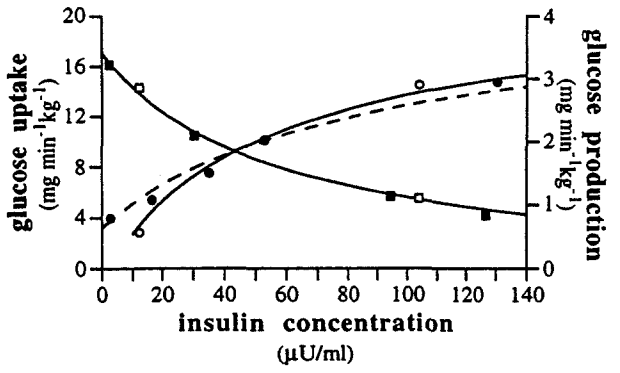

Fig 6. Dose-response curves for glucose uptake (circles and left scale) and production (squares and right scale). Closed symbols, data from Bradley et al.[28] Open symbols, data from this study. Solid lines are obtained with Eq 2 and the parameters estimated herein (for uptake, the point at ~3 μU/mL was excluded). The broken line is obtained with Eq 2 and the parameters from Bradley et al.[28]

Arteriovenous Differences

Hepatic glucose production calculated with the arteriovenous-difference method in the basal (−30 to 0 minutes) and insulin-stimulated (150 to 180 and 300 to 330 minutes) states was 3.1 ± 0.5, 0.48 ± 0.20, and 0.07 ± 0.19 mg · min^{-1} · kg^{-1}, respectively ($P \leq .05$, 150 to 180 and 300 to 330 minutes v basal). During the same periods, hepatic glucose uptake was 0.23 ± 0.26, 0.91 ± 0.27, and 0.96 ± 0.26 mg · min^{-1} · kg^{-1} (the increase did not reach statistical significance).

We found slightly higher values for glucose production with the circulatory model than with the arteriovenous-difference method during the quasi–steady-state periods of the clamp. Model-calculated glucose production was in fact 1.1 ± 0.3 and 0.8 ± 0.3 mg · min^{-1} · kg^{-1} for the periods 150 to 180 and 300 to 330 minutes, respectively ($P < .05$, model v arteriovenous differences). Glucose production calculated with the two methods in the three quasi–steady-state periods was highly correlated ($r = .89$, $P < .0001$, all periods and cases pooled).

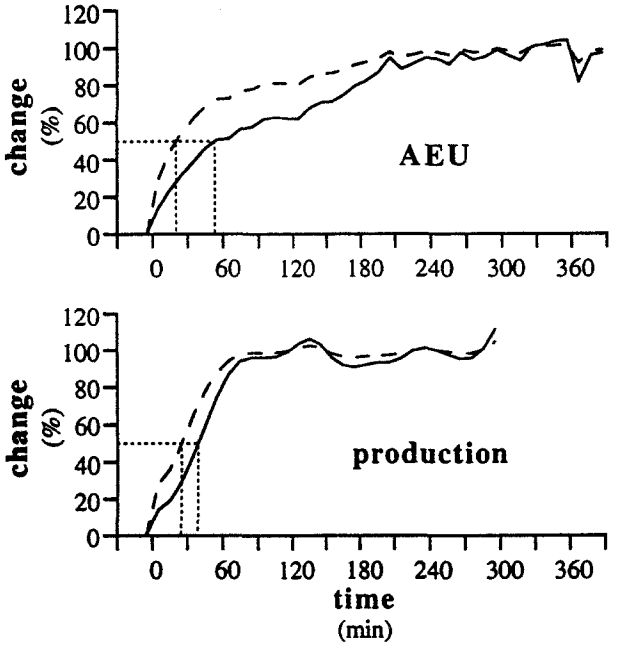

Fig 7. Rates of arterial-equivalent glucose uptake (AEU, top) and glucose production (bottom) expressed either as a % of the maximal change in the variable over the absolute basal rates (broken lines) or as a percent change of the insulin signal calculated with nonlinear transformation (solid lines). Dotted lines show calculation of the half-times.

DISCUSSION

In the present study, we used a novel circulatory modeling approach to assess the time course of insulin-stimulated glucose uptake during a euglycemic-hyperinsulinemic clamp. Although the problem of accurately assessing glucose production in this experimental condition has been satisfactorily solved by reducing the changes in specific activity,[2] the problem of the calculation of uptake has not been specifically addressed. The assumption of previous studies using Steele's model was that uptake is always equal to total Ra during a euglycemic-hyperinsulinemic clamp. Our results demonstrate that this assumption is likely incorrect. Glucose uptake increases faster than the total Ra of glucose during the initial 30 minutes of the clamp.

To reach this conclusion, we used an approach based on circulatory models that was specifically developed for addressing the problem of uptake.[11] The difficulty is that the determination of glucose uptake in the non–steady state is model-dependent, and thus requires an appropriate model. In addition, it is impracticable to perform validation experiments. Validation experiments require a direct measure of uptake, which cannot be directly measured in vivo. The use of arteriovenous-difference techniques across tissues does not help as it does for glucose production, because the delay as glucose is removed from the plasma pool to the site of uptake is unknown. Another approach would be to directly assess the time course of the total-body glucose mass and calculate the uptake (uptake = Ra − $d$mass/dt). This is also not feasible in vivo. Therefore, only an appropriate model choice can ensure a reliable calculation of uptake.

The approach we adopted has the advantage of being based on a physical description of the system (the circulatory loop) and on the application of Zierler's model-independent kinetic methods,[15,16] appropriately extended.[11,17] Circulatory models do not postulate a system structure (apart from the circulatory loop), but only make use of impulse responses (the so-called black-box approach). Assumptions are necessary to numerically calculate the artery-vein SPIR of the body tissues in our specific experimental condition,[18] but we do not assume a physical structure of body organs included in the periphery block of Fig 2. With circulatory models, the model dependency of the calculation of uptake is formalized on the basis of impulse responses. A clear distinction is made between the artery-vein impulse response, the determination of which does not require structural assumptions, and the artery-uptake impulse response, for which the determination requires knowledge of the system structure. This distinction naturally leads to a two-step calculation of uptake.[11] First, the so-called arterial-equivalent uptake is calculated (this step requires the artery-vein impulse response only), and then uptake can be predicted if some information is available on the artery-uptake impulse response.

In our experiments, we determined the artery-vein impulse response [$r_{per}(t)$], but did not attempt to derive the artery-uptake impulse response from $r_{per}(t)$. We instead addressed the simpler problem of obtaining an estimate of the mean artery-uptake transit time, using independent experimental information. The hypothesis we made extrapolating from published results (see the methods) is that the overall change of whole-body glucose mass during the clamp is negligible. Given our experimental results, the consequence of this hypothesis is that the unknown mean artery-uptake transit time (MTT_{AU}) was assumed to equal the computable mean artery-vein transit time (MTT_{AV}). We used this estimate of MTT_{AU} to predict uptake qualitatively, because uptake is delayed with respect to arterial-equivalent uptake, and MTT_{AU} is the delay.[11]

It is important to stress the difference between compartmental analysis and the circulatory model that we used. Compartmental analysis postulates a system structure when a specific model configuration is adopted, as in Ferrannini et al.[30] This is equivalent to assuming a relationship between the artery-vein and artery-uptake impulse responses, particularly between MTT_{AV} and MTT_{AU}.[17] Since compartmental models are not derived from a physical model, the analysis of uptake may be totally unreliable. The calculation of glucose uptake with compartmental models is thus essentially dependent on discretionary assumptions.[4] In contrast, our approach deliberately avoids postulating a relationship between the artery-vein and artery-uptake impulse responses. Only the mean transit time is estimated, and it is estimated using independent experimental evidence.

With the circulatory model, we demonstrated that during the initial 30 minutes of a euglycemic-hyperinsulinemic clamp the increase in uptake preceded the increase in the total Ra by about 4 to 5 minutes. The total Ra underestimated uptake by a maximum of 15% to 20% (1 to 1.5 $mg \cdot min^{-1} \cdot kg^{-1}$). Thus, assuming that the Ra of glucose is equal to uptake, as Steele's model does, leads to a systematic initial underestimation of uptake. This error is present even when the total Ra is calculated correctly with Steele's model by minimizing the changes in glucose specific activity. If the specific activity is allowed to decrease during the clamp, the error in estimating uptake using Steele's model is even greater. Although it is obvious that the error is negligible after the initial 30 minutes (during the latter part of the clamp, the equivalence of uptake and total Ra can be assumed), this error will affect assessment of the speed that insulin stimulates uptake. And it certainly prevents detection of the initial transient decrease of glucose mass observed in our experiments.

An equally important aspect in assessing the speed with which insulin activates a metabolic process is the scaling method used. In the traditional analysis, all variables are normalized to a homogeneous scale (usually 0% to 100%) by linear transformation (ie, linear scaling). For instance, the increment of glucose uptake over the basal value is expressed as a percentage of the maximal increment during the clamp. This time course can then be compared with an analogous calculation made on the plasma insulin concentration (eg, Ader et al[6]) or other physiological event such as activation of an enzyme.[10] This approach is only correct if the relationship between variables is linear. The relationship between insulin concentration and glucose uptake (and glucose production) is not linear. It exhibits saturation (ie, glucose uptake does not increase indefinitely as insulin levels are increased). As explained in the methods, the imposition of linear scaling on nonlinear data has the effect that as the dose of insulin is increased the apparent half-times for stimulation of glucose uptake (and suppression of glucose production) decrease. This is depicted using simulated data in Fig 8. In the simulation, the insulin signal that stimulates glucose uptake (ie, insulin concentration at the cell membrane) is supposed to increase monoexponentially from a basal to a maximal value as a consequence of a step-increase in plasma insulin concentration. The increase of the insulin signal is supposed to be proportional to the increase of plasma insulin concentration. The half-time of the insulin signal is supposed to be independent of the insulin level, and is fixed at 50 minutes. Glucose uptake is calculated assuming that it is related to the insulin signal according to the nonlinear function represented by Eq 2 and using the parameters of Eq 2 reported in the results. Glucose uptake is plotted in Fig 8 using the standard linear transformation. The simulation is repeated for the range of insulin concentration increments shown in Fig 8. The apparent half-time for stimulation of glucose uptake decreases as insulin concentration increases. Furthermore, even at 100 μU/mL, one has the impression that stimulation of glucose uptake (half-time, ~35 minutes) precedes activation of the stimulus, ie, the insulin signal (half-time, 50 minutes), which is a contradiction. However, if we calculate (as explained in the methods) the term we call the insulin signal from the glucose flux data using the inverse of Eq 2 and plot its time course using the standard linear transformation, we obviously reobtain the original insulin signal that has a dose-independent half-time of 50 minutes. In summary, our analysis shows that linear scaling of nonlinearly related variables may bias the assessment of the half-times of the variables. Both the dose dependency of half-times[9] and unexpected temporal relationships between two variables[10] can be a consequence of inappropriate linear scaling.

Using the traditional approach to assess the speed of onset of insulin action, we observed a half-time for the activation rate (20 minutes) similar to that reported by others in dog (15 to 30

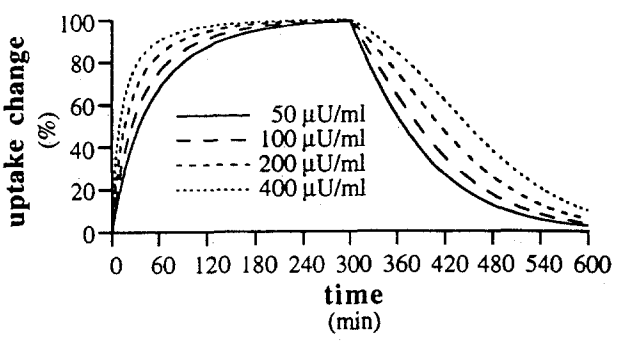

Fig 8. Simulated time course of the glucose uptake change expressed as % of the maximal change over basal at different insulin doses. The simulation includes an activation (0 to 300 minutes) and a deactivation (300 to 600 minutes) period. The insulin signal increases monoexponentially from the basal to the maximal value reported in the figure, and then returns to basal. The half-time of the insulin signal is 50 minutes for all insulin doses. The 4 curves are obtained with Eq 2 using the parameters estimated in this study.

minutes[6,28]). When we accounted for saturation by first normalizing the nonlinear glucose uptake data with the known relationship between insulin levels and glucose uptake (Eq 2), we found a markedly higher value for the half-time of the insulin signal controlling uptake, ie, 54 minutes. Such a difference markedly alters the perception of the temporal relationship between uptake and the physiological variables (eg, enzyme activation and protein phosphorylation).

The higher the prevailing insulin concentration compared with EC_{50}, the greater the degree of saturation and the shorter the apparent half-time (Fig 8). The EC_{50} value thus critically determines the half-time difference between the classic approach and that accounting for saturation. Our estimate of EC_{50} for uptake is about 55 μU/mL, which is lower than previously reported[28] (86 μU/mL). However, Fig 6 shows that the parameters of Eq 2 previously reported[28] do not adequately describe the curvature of the insulin-uptake relationship. In particular, glucose turnover at basal insulin levels predicted by these parameters is about 5.5 $mg \cdot min^{-1} \cdot kg^{-1}$, which is almost twofold the basal glucose turnover in a dog (~3 $mg \cdot min^{-1} \cdot kg^{-1}$). Furthermore, the increase of uptake that we have observed with an insulin concentration about 2.5 times higher than that of the present experiments does not appear compatible with a value of EC_{50} as high as that previously reported[28] (unpublished observations, June 1985). Therefore, although it may be difficult to estimate EC_{50} accurately, there is evidence that the system is driven into the saturation region at the insulin level we and several other groups have used to assess the timing of insulin action.[6,9,10,28,31] Since in these studies the investigators did not account for saturation, the timing of insulin action likely had not been properly evaluated. This possibility is confirmed by examination of the published plots of uptake in dogs and humans[6,9,28,31] that indicate a reduction of the half-times as the insulin level is increased (ie, driven toward saturation). The same mechanism can explain why at pharmacological insulin levels (>5,000 μU/mL) but not at moderate insulin concentrations (between 50 and 130 μU/mL) the estimate of uptake markedly preceded the time course of lymph insulin concentration.[6] The recent finding that the increase of glucose uptake preceded the increase of insulin receptor tyrosine kinase activity,[10] which is not logical, can also be explained by this phenomenon.

The influence of saturation on the apparent half-times becomes important when different populations are compared (such as in Prager et al[9] and Castillo et al[32]), because half-time differences can result simply from different dose-response curves. For example, obese subjects have been reported to have longer half-times than lean subjects.[32] This difference may be explained by a different degree of saturation in the two groups, since it is known that in obesity the EC_{50} for uptake may be increased.[33]

An even more complex problem is the interpretation of the speed of activation versus deactivation of glucose fluxes. Because of saturation, the apparent half-time decreases during activation and increases during deactivation (Fig 8). Thus, activation and deactivation profiles can be nonsymmetrical despite a symmetrical insulin signal. This phenomenon is clearly visible at pharmacological insulin levels,[6] and can also explain part of the difference between activation and deactivation profiles observed at lower insulin levels.[9] Furthermore, by comparing the half-times of onset and offset, the error on uptake of Steele's model may be more important, because different errors are expected in the activation and deactivation phase.

In summary, with our novel modeling approach, we have evaluated for the first time the impact of the error in estimating glucose uptake using Steele's model during a hyperinsulinemic-euglycemic glucose clamp. We have shown that the magnitude of the error is small in a relative sense, although Steele's model prevents detection of transient changes of glucose mass during the clamp. However, we found that a more important error is the classic method of comparing insulin concentration and glucose uptake and production on the same scale using a linear transformation. We have shown that because saturation has not been considered in previous studies, the speed of onset of insulin action may have been previously overestimated. Therefore, the interpretation of onset and offset curves obtained with the traditional analysis may require a revision.

APPENDIX

The circulatory model of Fig 2 was mathematically described according to the following steps[18]: (1) the impulse responses of the heart-lung and periphery blocks were modeled as multiexponential functions; (2) these impulse responses were converted to linear differential equations, which are more suitable for computer simulation; and (3) the differential equations of the heart-lung and periphery blocks were combined to obtain the differential equations of the circulatory model of Fig 2. These steps are described in detail in the first section of this Appendix. The second section illustrates the parameter estimation procedures.

Model Equations

Heart-lung block impulse response. The impulse response of the heart-lung block [$r_{lung}(t)$] was modeled with a two-exponential function. This impulse response was derived from studies on glucose kinetics in the heart-lung system.[21-23] The following assumptions were made: the glucose fractional extraction is zero (the coronary circulation is included in the periphery); the glucose volume (lung plus heart chambers) is V_{lung} = 17 mL/kg; and $r_{lung}(t)$ is initially zero, rapidly increases to a peak, and then more slowly returns to zero. Cardiac output (CO), expressed as blood flow, was assumed to equal 120 $mL \cdot min^{-1} \cdot kg^{-1}$.[19] Since glucose was measured in plasma and is carried in the red blood cells at a lower concentration, the cardiac output based on blood flow was corrected by the average ratio of blood glucose to plasma glucose concentration observed in dog (0.73[12]). The corrected value was thus $CO = 0.73 \times 120$ $ml \cdot min^{-1} \cdot kg^{-1}$.

The two-exponential $r_{lung}(t)$ was represented as the convolution of a faster and a slower monoexponential function,

$$r_{lung}(t) = \beta e^{-\beta t} \otimes \omega e^{-\omega t}, \quad \text{(A1)}$$

where the symbol $\otimes$ denotes the convolution operator, β is the exponent of the fastest exponential, and ω is the exponent of the slowest exponential. The convolution with the fastest exponential $\beta e^{-\beta t}$ has the effect of changing the initial brisk increase that a simple monoexponential response $\omega e^{-\omega t}$ would have at time zero into a rapid but gradual increase, as observed experimentally.[21] The initial value of $r_{lung}(t)$ is thus zero. The parameter β, which determines the initial rate of increase of $r_{lung}(t)$, was fixed to 15 min^{-1} to match previous experimental observations.[21]

The fact that both monoexponential functions in Eq A1 are of the type $\kappa e^{-\kappa t}$ ensures that their integral from zero to infinity is equal to 1 (the integral from zero to infinity of $e^{-\kappa t}$ is κ^{-1}). This also implies that the integral from zero to infinity of $r_{lung}(t)$, ie, the area under $r_{lung}(t)$, is equal to 1 (areas multiply with convolution). Thus, the fractional extraction of glucose (ie, 1 − area under the impulse response) is zero in the heart-lung block.

The parameter ω was determined from the mean transit time of $r_{lung}(t)$. This mean transit time equals the ratio between the volume of distribution of glucose in the lung-heart block and cardiac output,[24] ie, V_{lung}/CO, which is fixed (as already shown). The mean transit time of $r_{lung}(t)$ is equal to the sum of the mean transit times of $\beta e^{-\beta t}$ and $\omega e^{-\omega t}$ (mean transit times add up with convolution of functions with unit area). Since the mean transit time of a function of the type $\kappa e^{-\kappa t}$ is κ^{-1},[24] the mean transit time of $r_{lung}(t)$ is $\omega^{-1} + \beta^{-1}$. Thus, ω was calculated from the equation, $\omega^{-1} + \beta^{-1} = V_{lung}/CO$, ie,

$$\omega = \frac{\beta CO}{\beta V_{lung} - CO}. \tag{A2}$$

Using these assumptions, ω was calculated from Eq A2 and the mean transit time was calculated as V_{lung}/CO. The calculated values for ω and mean transit time were 7.85 min^{-1} and 11.6 seconds, respectively. The heart-lung impulse response was determined from these assumptions and was assumed to remain constant during the course of the study.

Periphery block impulse response. The impulse response of the periphery block $[r_{per}(t)]$ was modeled with a three-exponential function. This impulse response starts from zero, rapidly increases to a peak, and then gradually returns to zero according to a two-exponential pattern. Similarly to $r_{lung}(t)$, $r_{per}(t)$ was obtained from the convolution of a fast monoexponential function with a two-exponential function, ie,

$$r_{per}(t) = \gamma e^{-\gamma t} \otimes [A_1 e^{-\alpha_1 t} + A_2 e^{-\alpha_2 t}], \tag{A3}$$

where γ is the exponent of the fastest exponential, which determines the initial increase of $r_{per}(t)$, and α_1 and α_2 are the exponents of the decaying exponentials. Since the glucose distribution volume in the periphery block is greater than in the heart-lung block, a slower response is expected in the periphery than in the heart-lung block (ie, $\gamma < \beta$). Thus, the exponent γ was fixed to a value of 10 min^{-1}.

For convenience, Eq A3 was expressed with different parameters,

$$r_{per}(t) = \gamma e^{-\gamma t} \otimes [w\alpha_1 e^{-\alpha_1 t} + (1 - w)\alpha_2 e^{-\alpha_2 t}]\xi, \tag{A4}$$

where the parameters ξ and w ($0 < w < 1$) replace A_1 and A_2 [$A_1 = \xi w\alpha_1$ and $A_2 = \xi(1 - w)\alpha_2$]. The new parameters better characterize the impulse response $r_{per}(t)$. The integral from zero to infinity of $r_{per}(t)$, ie, the area under $r_{per}(t)$, is called the transmission,[24] and is equal to 1 − fractional extraction of $r_{per}(t)$. This integral equals the integral from zero to infinity of the two-exponential function $[w\alpha_1 e^{-\alpha_1 t} + (1 - w)\alpha_2 e^{-\alpha_2 t}]\,\xi$, because the integral from zero to infinity of $\gamma e^{-\gamma t}$ is 1 (areas multiply with convolution). Thus, the transmission is $[w + (1 - w)]\,\xi = \xi$ (the integrals from zero to infinity of $\alpha_1 e^{-\alpha_1 t}$ and $\alpha_2 e^{-\alpha_2 t}$ are equal to 1), and w represents the percent contribution of the first exponential to the total area under $r_{per}(t)$.

Differential equations. The impulse responses characterize the relationship between tracer concentration at the inlet and at the outlet of each of the blocks of Fig 2. Tracer concentration at the outlet is the convolution between the impulse response and tracer concentration at the inlet. For instance, arterial tracer concentration is the convolution between $r_{lung}(t)$ and tracer concentration in the right atrium. It was convenient to describe these convolution relationships with linear differential equations instead of convolution integrals, because differential equations are more suitable for computer simulation. With exponential impulse responses, the differential equations that describe convolutions have a relatively simple form. If y(t) denotes the result of the convolution between u(t) and the monoexponential impulse response $Ae^{-\alpha t}$, ie, $y(t) = Ae^{-\alpha t} \otimes u(t)$, y(t) is obtained from the differential equations,

$$\dot{x}(t) = -\alpha x(t) + u(t) \qquad \text{and} \qquad y(t) = Ax(t), \tag{A5}$$

where the dot denotes the time derivative and x(t) is an auxiliary variable, usually called a state variable (there are as many x(t) as the exponential terms of the impulse response). Note that no physical meaning can be attached to the auxiliary variables x(t).

The arterial tracer concentration, $G_a(t)$, is the convolution between $r_{lung}(t)$ and tracer concentration in the right atrium, $G_{ra}(t)$ [$G_a(t) = r_{lung}(t) \otimes G_{ra}(t)$]. Since $r_{lung}(t)$ was represented as a convolution of two monoexponential functions (Eq A1), $G_a(t)$ was obtained with a cascade convolution with two monoexponential functions [$G_a(t) = r_{lung}(t) \otimes G_{ra}(t) = \beta e^{-\beta t} \otimes \omega e^{-\omega t} \otimes G_{ra}(t)$]. Application of the principle of Eq A5 to the heart-lung block yields the differential equations,

$$\dot{x}_1(t) = -\omega x_1(t) + G_{ra}(t), \qquad \dot{x}_2(t) = -\beta x_2(t) + \omega x_1(t), \qquad \text{and} \qquad G_a(t) = \beta x_2(t), \tag{A6}$$

where the two equations account for the two monoexponential functions that constitute $r_{lung}(t)$ (Eq A1). Note that in the cascade convolution the y(t) (Eq A5) of the first equation, ie, $\omega x_1(t)$, becomes the u(t) of the second equation.

Similarly, the mixed-venous tracer concentration (ie, tracer concentration in the right atrium, not including the contribution of exogenous tracer infusion), $G_v(t)$, is the convolution between $r_{per}(t)$ and arterial tracer concentration, $G_a(t)$ [$G_v(t) = r_{per}(t) \otimes G_a(t)$]. Since $r_{per}(t)$ was represented as a convolution (Eq A4), this was also a cascade convolution [$G_v(t) = r_{per}(t) \otimes G_a(t) = \gamma e^{-\gamma t} \otimes [w\alpha_1 e^{-\alpha_1 t} + (1 - w)\alpha_2 e^{-\alpha_2 t}]\,\xi \otimes G_a(t)$], and was represented with the differential equations,

$$\dot{x}_3(t) = -\alpha_1 x_3(t) + w\xi G_a(t), \qquad \dot{x}_4(t) = -\alpha_2 x_4(t) + (1 - w)\xi G_a(t), \qquad \dot{x}_5(t) = -\gamma x_5(t) + \alpha_1 x_3(t) + \alpha_2 x_4(t), \qquad \text{and} \qquad G_v(t) = \gamma x_5(t), \tag{A7}$$

where the first two equations correspond to the two-exponential function $[w\alpha_1 e^{-\alpha_1 t} + (1 - w)\alpha_2 e^{-\alpha_2 t}]$ ξ in Eq A4 (the term $\alpha_1 x_3(t) + \alpha_2 x_4(t)$ is the convolution between $G_a(t)$ and this two-exponential function) and the last two equations account for the monoexponential function $\gamma e^{-\gamma t}$ in Eq A4.

The tracer concentration in the right atrium, $G_{ra}(t)$, can be expressed as a function of the mixed-venous concentration, $G_v(t)$, and the tracer infusion rate, $R_{inf}(t)$, using Fick's principle:

$$G_{ra}(t) = G_v(t) + R_{inf}(t)/CO. \tag{A8}$$

Using this equation, $G_{ra}(t)$ and $G_v(t)$ can be eliminated from Eqs A6 to A7, thus obtaining five differential equations (two for the heart-lung and three for the periphery block) that describe the circulatory model of Fig 2. These differential equations describe the whole-body response, and are used to calculate the model-predicted arterial tracer concentration, $G_a(t)$, that corresponds to the given tracer infusion rate, $R_{inf}(t)$. The parameters in the differential equations that must estimated are α_1, α_2, w, and ξ (ω, β, and γ are fixed). These parameters are time-varying during the clamp, and are modeled as detailed below.

Time-varying parameters. The parameters α_1, α_2, w, and ξ were held constant in the basal period, but were allowed to vary with time during the non–steady-state period. They gradually approached a new constant value by the end of the experiment. The parameter change was modeled as an exponential transition to the final steady-state value plus a linear drift, and was approximated with a piecewise constant function. This function had a constant value during the whole basal period (−150 to 0 minutes) and in each of the 39 time intervals of length t = 10 minutes [0, 10], [10, 20] . . . [(k − 1)T, kT] . . . [380, 390] minutes) into which the non–steady-state period was subdivided. For instance, w(t) was given by

$$w(t) = \begin{cases} w_b, & -150 \le t < 0 \\ w_k = w_b + \Delta w[(1 - e^{-\lambda kT}) + \mu kT], & (k-1)T \le t < kT, \quad k = 1 \ldots 39, \end{cases} \tag{A9}$$

where w_b is the basal value of w(t), and $w_1 \ldots w_{39}$ are the values of w(t) during the non–steady state. The parameter Δw determines the change of w(t) from the basal to the insulin-stimulated state, λ is the exponent of the exponential transition, and μ is the coefficient of the linear drift. The coefficients $\alpha_1(t)$ and $\alpha_2(t)$ were modeled with functions analogous to Eq A9.

During the non–steady state, the transmission $\xi(t)$ was modeled as a combination of a smooth component $[\theta(t)]$, represented by a function analogous to Eq A9, and a random component $[\epsilon(t)]$. The term $\epsilon(t)$ makes the fractional extraction $[1 - \xi(t)]$, the most important time-varying parameter, free from rigid functional constraints. As with the other time-varying coefficients, $\xi(t)$ was approximated with a piecewise constant function with values $\xi_b, \xi_1, \ldots, \xi_{39}$. The k-th value ξ_k was related to the corresponding values of the smooth and random components, θ_k and ϵ_k, by the equation

$$\xi_k = \theta_k(1 + \epsilon_k), \qquad k = 1 \ldots 39. \tag{A10}$$

In this way, $\epsilon(t)$ represents a relative deviation of $\xi(t)$ from the smooth component $\theta(t)$. During the basal period, the basal transmission ξ_b coincides with θ_b, ie, $\epsilon(t)$ is zero.

Glucose production was modeled as a piecewise constant function over the same set of time intervals on which the other time-varying model parameters were defined (Eq A9). Glucose production was thus determined by a vector of 40 parameters, p_b (basal production) and $p_1 \ldots p_{39}$ (production during the clamp). No functional constraint was imposed.

Parameter Estimation

The differential equations of the circulatory model, obtained by combining Eqs A6 to A10, represent the relationship between the known tracer infusion rate and arterial tracer concentration. The model-predicted tracer concentration was calculated by numerical simulation of the differential equations. The model parameters were determined using least squares, ie, by iteratively adjusting their values until the model-predicted tracer concentration matched the measured tracer concentration satisfactorily.

The parameters of the circulatory model that were estimated were as follows: λ and μ, which determine the time course of $\alpha_1(t)$, $\alpha_2(t)$, w(t), and $\theta(t)$ (a unique λ and μ value for all four functions); α_{1b}, α_{2b}, w_b, $\theta_b = \xi_b$, $\Delta\alpha_1$, $\Delta\alpha_2$, Δw, and $\Delta\theta$, which determine the values of $\alpha_1(t)$, $\alpha_2(t)$, w(t), and $\theta(t)$ in the basal and insulin-stimulated steady state; and the 39 elements of the vector ϵ and the 40 elements of the glucose production vector.

Model simulation and parameter estimation were performed with MatLab[34] on a VAX 4000/500 computer. Parameters were estimated with nonlinear weighted least squares, using a Levenberg-Marquardt minimization algorithm. Tracer data were analyzed first. The constant parameters in the basal steady state (α_{1b}, α_{2b}, w_b, and ξ_b) were estimated in a first analysis using the basal data (from −150 to 0 minutes). The time-varying parameters in the non–steady state (λ, μ,$\Delta\alpha_1$, $\Delta\alpha_2$, Δw, $\Delta\theta$, and $\epsilon_1 \ldots \epsilon_{39}$) were obtained in a second analysis using the data from 0 to 390 minutes and the steady-state parameters estimated in the first analysis.

Estimation of the 39 elements ϵ_k required constraints to avoid spurious oscillations of $\epsilon(t)$, as in deconvolution problems. Minimizing the sum of the weighted squared model residuals (observed minus model-predicted tracer concentration) using ordinary least squares would produce large fluctuations of $\epsilon(t)$ and data overfitting. Thus, the sum of the weighted squared model residuals plus the sum of the squared elements ϵ_k multiplied by a weighting factor was minimized instead. As this weighting factor is increased from zero, the spurious oscillations of $\xi(t)$ disappear and $\xi(t)$ tends to its regular component (θ_k, Eqs A9 to A10). The weighting factor was adjusted to make the model residuals unbiased and close, on average, to the expected measurement error.

After all of the model parameters were determined from the tracer, the component of glucose concentration at each sampling point due to the exogenous infusion of unlabeled glucose was calculated using the model. These glucose values were subtracted from the measured glucose concentrations, obtaining the concentration component due to endogenous production. Glucose production was estimated from this concentration component with a deconvolution-like approach.

Estimation of the 40 elements of glucose production (p_b, $p_1 \ldots p_{39}$) required constraints, and a procedure analogous to that used for $\epsilon(t)$ was followed. Glucose production was estimated by minimizing the sum of the weighted squared model residuals (observed minus model-predicted

endogenous tracee concentration) plus the sum of the squared elements of the second derivative of glucose production (calculated by finite differences) multiplied by a weighting factor. As this weighting factor is increased from zero, the spurious oscillations of glucose production disappear and glucose production tends toward a linear function of time. The weighting factor was adjusted to make the model residuals unbiased and close, on average, to the expected measurement error.

REFERENCES

1. Steele R: Influences of glucose loading and of injected insulin on hepatic glucose output. Ann NY Acad Sci 82:420-430, 1959
2. Bergman RN, Steil GM, Bradley D, et al: Modeling of insulin action in vivo. Annu Rev Physiol 54:861-883, 1992
3. Norwich KH: Measuring rates of appearance in systems which are not in steady state. Can J Physiol Pharmacol 51:91-101, 1973
4. Mari A: On the calculation of glucose rate of disappearance in nonsteady state. Am J Physiol 266:E825-E826, 1994 (letter)
5. Bergman RN, Steil GM: Reply to the letter "On the calculation of glucose rate of disappearance in nonsteady state" by A. Mari. Am J Physiol 266:E827-E828, 1994
6. Ader M, Poulin RA, Yang YJ, et al: Dose-response relationship between lymph insulin and glucose uptake reveals enhanced insulin sensitivity of peripheral tissues. Diabetes 41:241-253, 1992
7. Butler PC, Caumo A, Zerman A, et al: Methods for assessment of the rate of onset and offset of insulin action during nonsteady state in humans. Am J Physiol 264:E548-E560, 1993
8. Poulin RA, Steil GM, Moore DM, et al: Dynamics of glucose production and uptake are more closely related to insulin in hindlimb lymph than in thoracic duct lymph. Diabetes 43:180-190, 1994
9. Prager R, Wallace P, Olefsky JM: In vivo kinetics of insulin action on peripheral glucose disposal and hepatic glucose output in normal and obese subjects. J Clin Invest 78:472-481, 1986
10. Miles PDG, Levisetti M, Reichart D, et al: Kinetics of insulin action in vivo: Identification of rate limiting steps. Diabetes 44:947-953, 1995
11. Mari A: Calculation of organ and whole-body uptake and production with the impulse response approach. J Theor Biol 174:341-353, 1995
12. Adkins BA, Myers SR, Hendrick GK, et al: Importance of the route of intravenous glucose delivery to hepatic glucose balance in the conscious dog. J Clin Invest 79:557-565, 1987
13. Wide L, Porath J: Radioimmunoassay of proteins with the use of Sephadex-coupled antibodies. Biochim Biophys Acta 130:257-260, 1966
14. Leevy CM, Mendenhall CL, Lesko W, et al: Estimation of hepatic blood flow with indocyanine green. J Clin Invest 41:1169-1179, 1962
15. Meier P, Zierler KL: On the theory of the indicator-dilution method for measurement of blood flow and volume. J Appl Physiol 6:731-744, 1954
16. Zierler KL: Theory of the use of arteriovenous concentration differences for measuring metabolism in steady and non-steady states. J Clin Invest 40:2111-2125, 1961
17. Mari A: Circulatory models of intact-body kinetics and their relationship with compartmental and noncompartmental analysis. J Theor Biol 160:509-531, 1993
18. Mari A: Determination of the single-pass impulse response of the body tissues with circulatory models. IEEE Trans Biomed Eng 42:304-312, 1995
19. Ettinger SJ: Textbook of Veterinary Internal Medicine. Diseases of the Dog and Cat. Philadelphia, PA, Saunders, 1989, p 927
20. Baron AD: Hemodynamic actions of insulin. Am J Physiol 267:E187-E202, 1994
21. Perl W, Silverman F, Delea AC, et al: Permeability of dog lung endothelium to sodium, diols, amides, and water. Am J Physiol 230:1708-1721, 1976
22. Chinard FP: Exchanges across the alveolar-capillary barrier, in Fishman AP, Hecht HH (eds): The Pulmonary Circulation and Interstitial Space. Chicago, IL, The University of Chicago Press, 1969, pp 79-98
23. Meyer EC, Ottaviano R: Right lymphatic duct distribution volume in dogs. Relationship to pulmonary interstitial volume. Circ Res 35:197-203, 1974
24. Lassen NA, Perl W: Tracer Kinetic Methods in Medical Physiology. New York, NY, Raven, 1979
25. Katz A, Nyomba BL, Bogardus C: No accumulation of glucose in human skeletal muscle during euglycemic hyperinsulinemia. Am J Physiol 255:E942-E945, 1988
26. Yki-Jarvinen HK, Sahlin K, Ren JM, et al: Localization of rate limiting defect for glucose disposal in skeletal muscle of insulin-resistant type I diabetic subjects. Diabetes 39:157-167, 1990
27. Vaag A, Henrikson JE, Beck-Nielsen H: Decreased insulin activation of glycogen synthase in skeletal muscles in young nonobese caucasian first-degree relatives of young patients with non–insulin-dependent diabetes. J Clin Invest 89:782-788, 1992
28. Bradley DC, Poulin RA, Bergman RN: Dynamics of hepatic and peripheral insulin effects suggest common rate-limiting step in vivo. Diabetes 42:296-306, 1993
29. McGuinness OP, Fugiwara T, Murrell S, et al: Impact of chronic stress hormone infusion on hepatic carbohydrate metabolism in the conscious dog. Am J Physiol 265:E314-E322, 1993
30. Ferrannini E, Smith JD, Cobelli C, et al: Effect of insulin on the distribution and disposition of glucose in man. J Clin Invest 76:357-364, 1985
31. Katz H, Butler P, Homan M, et al: Hepatic and extrahepatic insulin action in humans: Measurement in the absence of non–steady-state error. Am J Physiol 264:E561-E566, 1993
32. Castillo C, Bogardus C, Bergman R, et al: Interstitial insulin concentrations determine glucose uptake rates but not insulin resistance in lean and obese men. J Clin Invest 93:10-16, 1994
33. Olefsky JM: Insulin resistance and insulin action. An in vitro and in vivo perspective. Diabetes 30:148-162, 1981
34. MATLAB Reference Guide. Natick, MA, The MathWorks, 1992